Progress in Surface Science 87 (2012) 23–45

Contents lists available at SciVerse ScienceDirect

Progress in Surface Science

journal homepage: www.elsevier.com/locate/progsurf

Review

Surfaced-enhanced cellular fluorescence imaging

Qi Hao [a], Teng Qiu [a,b,*], Paul K. Chu [b,*]

[a] Department of Physics, Southeast University, Nanjing 211189, China
[b] Department of Physics and Materials Science, City University of Hong Kong, Tat Chee Avenue, Kowloon, Hong Kong, China

ARTICLE INFO

Keywords:
Surface-enhanced spectroscopy
Surface plasmons
Cellular fluorescence imaging
Fluorescence microscopy
Plasmonic nanostructures

ABSTRACT

The novel and burgeoning technique of surfaced-enhanced cellular fluorescence imaging has tremendous potential in the monitoring and investigation of intracellular processes at the single-molecular level, for instance, high-resolution cellular imaging, long-term *in vivo* observation of cell trafficking, tumor targeting, and diagnostics. The success hinges on the development and fabrication of plasmonic nanostructured surfaces with size and shape compatible with cell interactions because they are crucial to enhanced cellular imaging. In this review, the mechanism of surface-enhanced cellular fluorescence imaging is discussed in view of metal-enhanced fluorescence. The design of nanostructured surfaces with evenly distributed plasmonic fields suitable for enhanced cellular fluorescence imaging such as nanoparticle superlattice coatings, lithographically-based substrates, and alumina-templated surface are described.

Contents

* Corresponding authors. Address: Department of Physics, Southeast University, Nanjing 211189, China and Department of Physics and Materials Science, City University of Hong Kong, Tat Chee Avenue, Kowloon, Hong Kong, China (T. Qiu), Department of Physics and Materials Science, City University of Hong Kong, Tat Chee Avenue, Kowloon, Hong Kong, China (P.K. Chu).
E-mail addresses: tqiu@seu.edu.cn (T. Qiu), paul.chu@cityu.edu.hk (P.K. Chu).

0079-6816/$ - see front matter © 2012 Elsevier Ltd. All rights reserved.
http://dx.doi.org/10.1016/j.progsurf.2012.03.001

1. Introduction

1.1. Conventional cellular fluorescence imaging methods and limitations

The history and development of fluorescence and associated techniques is replete with independent inventions spanning almost two centuries. In 1845, the first observation of fluorescence from a quinine solution was reported [1]. To describe the phenomenon and explain the mechanism, George Gabriel Stokes initially used the term "dispersive reflection" in his article "On the Change of Refrangibility of Light" in 1852 [2]. The 20th century witnessed ground breaking discoveries such as excitation spectrum of a dye (1905), fluorescence quenching (1919), fluorescence polarization in a dye solution (1923), determination of fluorescence yields (1924), direct measurement of nanosecond lifetime (1926), Jablonski diagram (1935), and quantum mechanical theory of dipole–dipole interactions (1948). These and other studies established the theoretical basis, and being highly-sensitive, specific and non-invasive, fluorescence techniques have been quickly adopted by scientists and engineers in many areas of molecular biology, chemistry, geology, gemology and so on. Consequently, related applications pertaining to analysis, sensing, lighting, equipment, dyes, and biological detection have been spawned [3–6].

These new fluorescence applications strongly promoted development of basic and applied life sciences including genomics, proteomics, bioengineering, medical diagnostics, and industrial microbiology [7–12]. At present, some relatively simple and convenient methods such as fluorescence resonance energy transfer [13], fluorescence lifetime imaging [14,15], fluorescence polarization-resolved imaging [15], and total internal reflection fluorescence [16,17] are commercially viable. These techniques not only render the detection and monitoring of protein activity in cells possible, but also provide sensitivity sufficiently high for medical diagnostics and genomics [18–21]. In addition, the development of fluorescent probes has spurred the studies of protein localization and functions in living cells. These fluorescent probes provide convenient markers in the *in vivo* study of gene expression and protein targeting in single cells and whole organisms [22]. These and other discoveries have revolutionized cell biology by allowing scientists to monitor molecular activities inside living cells in real time, that is, cellular imaging.

Cellular imaging is especially useful to non-invasive monitoring of diseases, evaluation of drug effects, assessment of the pharmacokinetic behavior of drugs, and identification of molecular biomarkers for diseases [23]. In order to accurately study the progress, a multi-color biological labeling method is needed for membrane protein imaging. Cellular fluorescence imaging meets the requirement due to the large range of fluorophores with distinctive spectral characteristics suitable for clinical practice. Moreover, it offers the specific, targeted imaging contrast needed for the study of specific cellular processes. Hence, cellular fluorescence imaging, particularly fluorescence microscopy, is now an irreplaceable tool in biomedical science. Fluorescence microscopy, which allows the detection of

single molecules, has good compatibility with living cells and is used in dynamic and minimally invasive imaging experiments. Many different fluorescent dyes can be used to stain various structures or chemical compounds [24]. One particularly powerful method is to couple a fluorophore such as fluorescein or rhodamine to antibodies in immunostaining. Fluorescent dyes can be chemically bound to antibodies and coupled to a specific protein in cells thereby providing microscopic contrast with high specificity [25].

Cellular fluorescence imaging methods can be used to quantify cellular phenotypic changes and investigate the role of a particular target in *in vitro* disease studies. Moreover, the advent of fluorescence microscopy and other sophisticated techniques has enabled routine studies of dynamic processes in living cells. These fluorescence techniques can deliver the necessary resolution to image certain cellular organelles and track proteins in for example, the nucleus, endoplasmic reticulum, and Golgi apparatus, and other biomolecules in living cells [26], so that valuable information about the dynamics of intracellular networks, signal transduction, and intercellular interactions can be obtained. Versatile fluorescence-based techniques, particularly confocal microscopy and wide-field microscopy, excel in cell imaging due to the flexible resolution and different magnification options [27]. Specially, methods such as magnetic resonance imaging and optical coherence tomography can provide real-time cellular imaging but can hardly achieve a resolution of less than $\sim$10 μm. By contrast, electron microscopy can provide almost molecular-level spatial resolution. However, dynamic imaging is not available by electron microscopy because this method is invasive. Between these two resolution extremes, fluorescence microscopy is better suited to cell imaging.

In spite of recent advances, the spatial and temporal resolution of cellular fluorescence microscopy is limited by traditional organic fluorescent dyes. When using fluorophores as dyes, the signal cannot be easily discerned [28,29] from the background of autofluorescence, which is natural emission from biological entities [30]. Autofluorescence can be problematic in fluorescence microscopy due to several reasons. First of all, the unwanted signals may interfere with specific fluorescent signals especially when the latter are very dim. Secondly, the emission lifetime on the order of 2–4 ns is very close to that of the cell autofluorescence background, and thirdly, organic fluorophores are known to emit signals with poor stability and strong blinking [31,32]. In many instances, the sensitivity is limited by autofluorescence from the sample rather than lack of signal. Hence, one of the main challenges is to improve the sensitivity and photostability.

1.2. Surfaced-enhanced cellular fluorescence imaging: a novel and burgeoning technique for cellular imaging

In order to further improve the sensitivity, there are continuous attempts to lower the detection limits. Detection of a fluorophore is usually limited by the quantum yield, autofluorescence from the sample, and photostability of the fluorophore. In addition, the complex milieu encountered inside living cells requires substantial adaptation of current *in vitro* techniques. Hence, in order to enhance the performance of existing imaging techniques, there is increasing use of metallic nanostructures to modify the spectral properties of fluorophores and to overcome some of these photophysical constraints.

As a spontaneous emission process, fluorescence involves the interaction between the emitter and its environment and is thus subjected to external factors [33]. It creates the possibility of tailoring the fluorescence process to increase the emission intensity [34]. In early studies on fluorophore-metal interactions in the 1970s [35,36], a fluorophore was used to interact with a smooth silver or gold film typically about 40 nm thick and the fluorescence intensity and lifetime were not altered dramatically. However, in contrast to a smooth metallic surface, rough surfaces seem to interact more strongly with light [37]. The generally accepted view is that intensity amplification arises mainly from the electric field enhancement that occurs in the vicinity of small (in relation to the light wavelength), interacting metal particles illuminated with light in resonance or near resonance with the localized surface-plasmon (SP) frequency of the metal structure. Silver or gold colloids are typically sprayed onto a substrate to obtain a suitable surface with the appropriate electromagnetic (EM) resonance or films with silver islands are produced by chemical means. Depending on the geometry and the distance between the metal and fluorophore, these surfaces can result in fluorescence enhancement by factors of up to

1000 [38,39]. Even though spraying silver or gold colloids onto a substrate produces high fluorescence signals from some local "hot spots", it is not easy to obtain reliable, stable, and uniform signals spanning a wide dynamic range from the metal surface due to particle aggregation. Hence, methods that can produce as evenly distributed nanoscale surface are necessary in order to make sure that different parts of the sample can have the same degree of amplification and enable the use of surfaced-enhanced cellular fluorescence imaging in the study of intracellular processes at the single-molecule level including high-resolution cellular imaging, long-term *in vivo* observation of cell trafficking, tumor targeting, and diagnostics. Nevertheless, although this technique boasts the aforementioned advantages, many issues are still not well understood and require more research, for instance, reproducible control of the nanoparticle-surface properties. Furthermore, the variable response of different cell types, nonspecific serum-protein adsorption on the nanoparticle surface, and different experimental conditions render systematic studies of surfaced-enhanced cellular fluorescence imaging challenging. Fortunately, recent advances in nanobiotechnology have made it an achievable and worthwhile goal. In this review, we discuss the mechanism and applications of surfaced-enhanced cellular fluorescence imaging and describe the different methods to produce plasmonic nanostructures to overcome the aforementioned problems. The advantages and limitations of existing techniques are summarized and ideas about further improvement are presented.

2. Mechanism of surface-enhanced cellular fluorescence imaging

2.1. Surface plasmons (SPs)

Metal-enhanced fluorescence is the major mechanism in surface-enhanced cellular fluorescence imaging. Studies about the effects of metallic particles and surfaces on fluorescence enhancement dated back to the reports of Drexhage in 1970 [35]. A fluorophore in the excited state has the properties of an oscillating dipole (Fig. 1) [40] and the excited fluorophore can induce electron oscillations in the metal. The electric field created by the metal can interact with the excited fluorophore and alter its emission. This interaction is bidirectional, so that light-induced oscillations in the metal can affect the fluorophore by offering decay channels. A reduced lifetime is found when the reflected field is in phase with the oscillating dipole of the fluorophore and conversely, an increase is observed when the reflected field is out of phase with the fluorophore dipole.

This discovery has spurred many subsequent theoretical and experimental studies on the interactions between the oscillating dipole and metallic surfaces/particles [41–45] and readers are referred to several excellent review articles for these important developments during this period [46–48]. It was found that nonradiative energy transfer to a nearby metal surface could be an effective decay channel for an excited molecule and there could be close connection between the dependence of this transfer rate and SP modes. More information and details can be found in the literature by others [33,49,50].

A surface plasmon (SP) is a quasi-particle due to quantization of plasma oscillations confined to the surface. SPs interact strongly with light near a metallic surface resulting in another quasi-particle called surface plasmon polariton which propagates along the surface of the metal. Sometimes, surface plasmon polaritons are also called SPs for convenience and we also use this abbreviation for surface

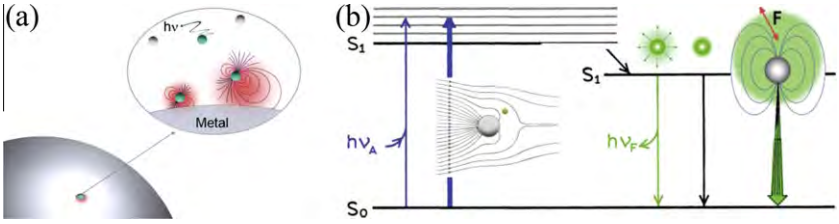

Fig. 1. (a) Fluorophore near a metallic surface. (b) Modified Jablonski diagram including the metal–fluorophore interactions. The bolder arrows represent increased rates of excitation and emission. Reprinted with permission from [40]. Copyright 2008 the Royal Society of Chemistry.

plasmon polaritons in the following discussion. SPs at the interface between a metal and dielectric materials have combined EM wave and surface charge characteristics. The EM wave has a transverse magnetic characteristic and the generation of surface charge requires an electric field normal to the surface. These two effects enhance the field component perpendicular to the surface near the surface and it decays exponentially with distance away from it [46]. The perpendicular field is evanescent or near-field in nature being a consequence of the bound, non-radiative nature of SPs because the wave vector of a polariton is normally larger than that of a free photon at the same frequency and prevents power from propagating away from the surface. Another important effect arising from the interaction between the surface charge density and EM field is the momentum of the SP mode, $\hbar k_{SP}$. Solving Maxwell's equations using the appropriate boundary conditions yields the SP dispersion relationship [51], that is, frequency-dependent SP wave-vector, k_{SP}, as:

$$k_{SP} = k_0 \sqrt{\frac{\varepsilon_d \varepsilon_m}{\varepsilon_d + \varepsilon_m}}.$$

The frequency-dependent permittivity of the metal, ε_m, and dielectric material, ε_d, must have opposite signs in order for SPs to be possible at the interface. This condition is satisfied on metals because ε_m is both negative and complex (the latter corresponding to absorption on the metal). The increase in momentum is associated with binding of the SPs to the surface, and the resulting momentum mismatch between the light and SPs with the same frequency must be bridged if light is to be used to generate SPs. To provide the missing momentum, we may make use of scattering from subwavelength protrusions or holes on the surface to generate SPs locally [52,53]. A periodic corrugation in the metal surface can also provide the momentum [54] and some other techniques are also available to solve this problem [55,56].

We now discuss how SPs propagate on the metal surface. After light has been converted into an SP mode on a flat metal surface, it will propagate but be gradually attenuated due to losses from absorption by the metal. The degree of attenuation depends on the dielectric function of the metal at the oscillation frequency of the SPs. A classical theoretical approach to calculate the relaxation processes induced by the modified environment presents accurate results on the process in the case of a planar interface [46,48]. However, if the flat metal surface is changed to a rough or corrugated one, the results can be difference. Calculation [57] demonstrates that absorption by the metal can be overcome when the surface is periodically textured on the scale of the light wavelength. This is important to fluorescence enhancement because it provides an effective way to maximize radiative relaxation as all relaxation channels compete with each other. Besides, silver exhibits the smallest loss in the visible spectrum and can lead to fluorescence enhancement. When the periodic length of the nanostructure is smaller than half of the effective wavelength, reduced absorption by the metal is observed together with strong localized SP resonance [58]. Simultaneously, the electric and magnetic fields can be localized thereby giving rise to an inhomogeneous EM field distribution that can be exploited in local EM enhancement [59]. The inhomogeneity can also be used to specifically excite a given fluorophore and constitutes one of the causes of large enhancement when coupled to SPs. All in all, localization of the EM near metal nanostructures and coupling to propagating modes can increase fluorescence by several orders of magnitude [49].

Based on the previous discussion, it can be inferred that near-field coupling between the emitter and surface modes plays a crucial role in metal-enhanced fluorescence. The near-field components provide resonant coupling between the fluorophore and metallic surface, resulting in large enhancement in the vicinity of metallic particles when the size is much smaller than the detected wavelength. By means of near-field transmission imaging and near-field two-photon excitation imaging, investigation of SPs on metal nanostructures can be conducted [60]. It is noted that plasmons are the results of quantization of classical plasma oscillations, and so most of their properties can be derived from Maxwell's equations. Thus it is possible to design specific surfaces with matching optical spectrum utilizing calculated results since the surface morphology of the materials determines the types of SPs [51]. Hence, the main challenge of surface-enhanced fluorescence imaging is thus to control and design surface structures to maximize the fluorescence enhancement of a fluorophore by adjusting the local electric field.

2.2. Surface-enhanced cellular fluorescence imaging

Fluorescence is a spontaneous emission process and the rate of relaxation is dictated by the coupling between the excited state of the molecule and vacuum oscillations in the surroundings. This can be reformulated in classical terms where the probability of photon emission is related to the photonic mode density [33]. As aforementioned, fluorophore emission can be modified by the EM boundary conditions near the fluorophore and so enhancement of fluorescence partly relies on the ability to tailor the local environment of the molecule to maximize the radiative relaxation rate compared to the same fluorophore in free space. This is accomplished by minimizing competitive non-radiative processes [49]. In most cases, it results in a reduction of the fluorescence lifetime and increase in the fluorescent intensity of the fluorophore. Several studies have been performed to study this issue [25,61–65] and it has been shown that the quantum yield is the most important characteristics of a fluorophore. Good coupling between the localized EM field and propagating modes enables successful competition with internal non-radiative decay of the emitter *via* emission of phonons into the materials immediately adjacent to the emitter. In this way, the low radiative quantum yield of emission may be enhanced [66]. The fluorescence quantum yield is defined as the ratio of the number of photons emitted to the number absorbed. Here, Γ describes the emission rate of the fluorophore or all the EM relaxation processes and k_{nr} represents the sum of all possible non-radiative decay rates. The quantum yield Q and lifetime τ are given by

$$Q = \frac{\Gamma}{\Gamma + k_{nr}}$$

and

$$\tau = \frac{1}{\Gamma}.$$

The presence of a nearby metallic surface can modify the radiative rate of an excited fluorophore. Supposing that a fluorophore is located at a given distance from a metallic surface and the radiative rate increase is given by Γ_m, the quantum yield (Q_m) of the fluorophore is given by

$$Q_m = \frac{\Gamma + \Gamma_m}{\Gamma + \Gamma_m + k_{nr}}.$$

Accordingly

$$\tau = \frac{1}{\Gamma + \Gamma_m}.$$

This equation suggests that high quantum yields can be accomplished when Γ_m is comparable to k_{nr}. Furthermore, these effects are larger for fluorophores with lower quantum yields and hence, low quantum field fluorophores can be enhanced by fabricating metallic particles with a suitable size and shape. Altering the distance is another important aspect to achieve maximum enhancement and it will be discussed in the next section. The process is termed radiative decay engineering because the increased radiative decay rate is perhaps the most unusual effect of a metallic surface [25]. It is unusual because this intrinsic rate which is determined by the extinction coefficient and the local refractive index is typically constant in a given fluorophore [67]. In radiative decay engineering, an increase in the radiative decay rate provides a unique way to increase the quantum yield while the lifetime decreases. It results in useful emission from weakly fluorescent molecules thereby offering the potential to image fluorophores with intrinsically low quantum yield in cells. By analyzing the equation shown above, the reduced lifetime is concurrent with increased decay rate. These changes increase the sensitivity and photostability while interference from unwanted background emission can be reduced. Relevant applications are thus being developed and the use of metal-enhanced fluorescence in cellular imaging, so-called surface-enhanced cellular fluorescence imaging, is a good example.

3. Design of surfaces suitable for enhanced cellular fluorescence imaging

3.1. Distance dependence

We have mentioned the first study about fluorescence enhancement was in 1970. However, researchers got little achievements in the next 20 years. The research on metal-enhanced fluorescence in this period was overshadowed by the large signal enhancements offered by surface-enhanced Raman scattering. Efficient Raman enhancement requires close contact between the molecules being studied and metallic surface and the typical distance is less than 2–3 nm. At this short distance, fluorescence of molecules is significantly quenched primarily by energy transfer to the metal surface. Fluorescence enhancements that are much smaller than those of the Raman signals have been observed [68]. Pockrand et al. [69] used momentum-matching techniques to determine the distance dependence of the coupling between the emitters and SPs and found a maximum coupling distance of approximately 20 nm. Knobloch et al. [70] also observed an optimum coupling distance for SPs using gratings to scatter SPs thus allowing the SPs decay channel to be monitored. In 1997, W. L. Barnes measured the decay time of a europium (Eu^{3+}) complex positioned at various distances from a planar silver mirror [71]. They investigated the distance dependence on the emission lifetime of Eu^{3+} ions in front of silver mirrors with thicknesses from 13 to 200 nm. The mirrors were coated with spacer layers of 22-tricosenoic acid using the Langmuir–Blodgett technique [72,73]. By varying the number of Langmuir–Blodgett layers, the emitter surface separation could be varied in a controlled way. By conducting lifetime measurements, they found that the spontaneous emission rate of Eu^{3+} could oscillate with both the distance and thickness of the silver mirror but the lifetime of the thinnest film displayed a different tendency. The fluorescence lifetime dropped dramatically for small metal - fluorophore distances [74], implying that spontaneous emission was quenched for small emitter-surface separations. They were also surprised to find that coupling between the emitter and SP mode was maximum for a small but finite separation between the emitter and surface. They attributed this phenomenon to the competition between the decay channels and surface waves. As the separation was reduced, the latter decay route became dominant.

A systemic explanation was proposed to explain this phenomenon [33]. Relaxation processes on flat metallic thin films have already been discussed earlier in this paper. The emitter interferes with the reflected EM waves and the spontaneous emission rate oscillates with increasing distances [75]. In the experiments conducted by W. L. Barnes, as the thickness of the Langmuir–Blodgett layers was increased, it was finally able to support a waveguide mode. The waveguide mode, like SPs, is a resonant optical mode of the system and may provide a new decay route for the excited molecule. As the thickness of the layer is increased, further waveguide modes may be supported by the structure thereby adding more decay channels. The coupling between excited molecules and waveguide modes is important to sensing applications [76], but in surface-enhanced cellular fluorescence imaging, this causes strong quenching of the fluorophores.

Several processes can result in fluorescence quenching [77,78]. There are three main physical quenching mechanisms, all involving excitation of an electron–hole pair [33]. Process A arises from the bulk and the excitation energy of the molecule is absorbed by the creation of an exciton in the substrate. Process B arises from the surface and the excitation energy is absorbed by the creation of an exciton in the surface. Process C arises from the spatial variation in the near field, which is related to the roughness of the nanostructured surface. Besides these mechanisms, fluorophores can form nonfluorescent complexes with quenchers and can be quenched by attenuation of the incident light or other absorbing species. A classical model allows one to observe and evaluate quantitatively each relaxation channel [46]. It implies that depending on the distance, metallic surfaces or particles can lead to either quenching or enhancement of fluorescence [49]. Commonly, strong quenching occurs at distances very close to the planar metallic surface, usually less than 10 nm, whereas enhancement generally occurs at tens of nanometers from the surface and is sensitive to the nanoscale roughness of the metal. However, it is difficult to predict precisely the optimal distance under a specific condition to obtain the maximum radiative decay rates because it varies with the type and surface roughness of the metal [79].

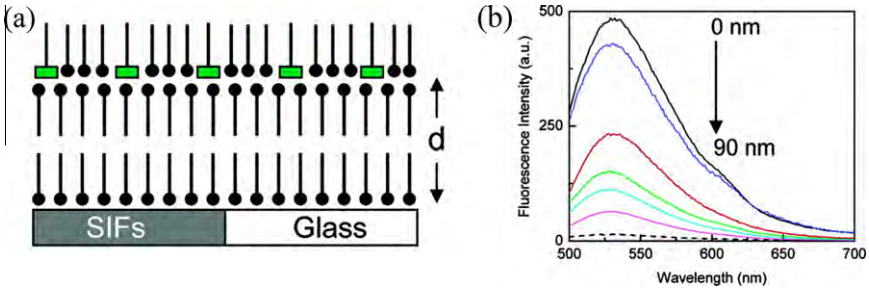

Fig. 2. (a) Schematic representation of a corresponding monolayer of the probes deposited on top of inert stearic acid layers on glass and silver island film surfaces. "d" is the distance between the fluorophore and silver island film surface that can be varied by the number of inert stearic acid layers at a resolution of ~2.5 nm. (b) Emission spectra of NBD-C18/stearic acid monolayers deposited at various distances from the silver island film surface. The fluorescence spectra of NBD-C18/ stearic acid on a glass surface are also included (–). Reprinted with permission from [80]. Copyright 2006 American Chemical Society.

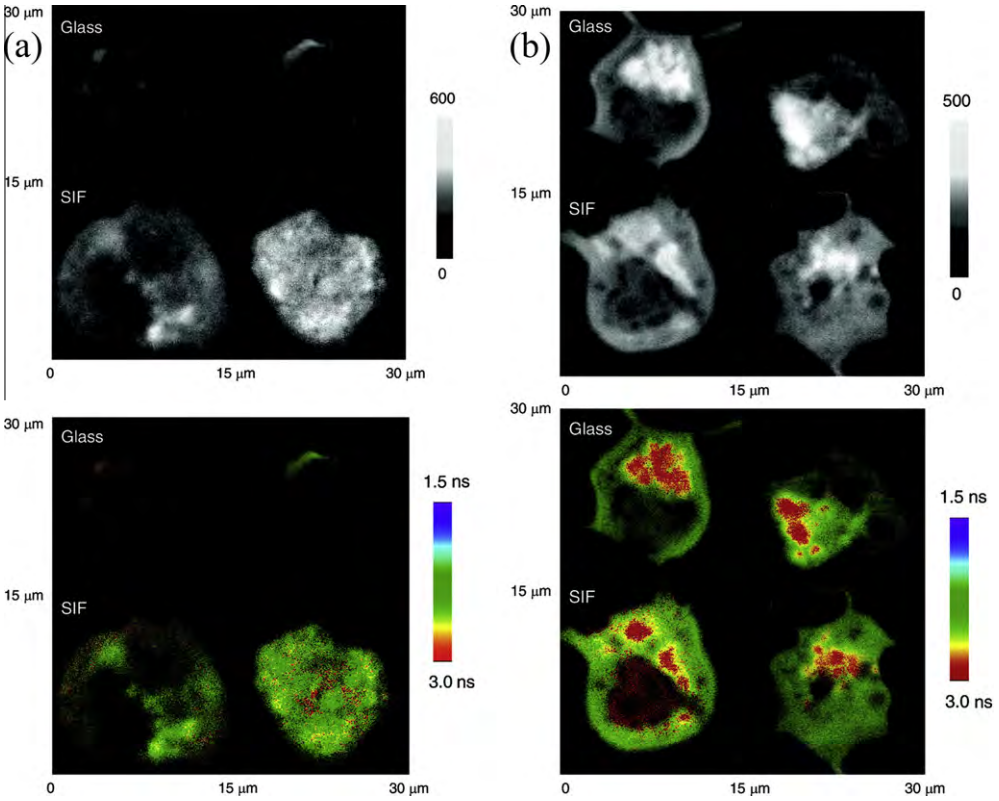

Fig. 3. (a) Upper panel: representative emission intensity images of PM1 cells labeled with Alexa Fluor 680–dextran conjugates adhered to the cell membranes on a glass slide and on silver island films. Lower panel: corresponding lifetime images of the intensity images in the upper panel. The scale of the diagrams is $15 \times 15\ \mu m^2$. The resolution is 400×400 pixels with an integration of 0.6 ms/pixel. (b) Upper panel: representative emission intensity images of PM1 cells labeled with YOYO bound in the cell nucleus on a glass slide and on silver island films. Lower panel: corresponding lifetime images of the intensity images in the upper panel. The scale of the diagrams is $15 \times 15\ \mu m^2$. The resolution is 400×400 pixels with an integration of 0.6 ms/pixel. Reprinted with permission from [82]. Copyright 2008 American Chemical Society.

Although these results provide better understanding of the distance dependence of metal-enhancement fluorescence, the spacing between the fluorophore and metallic surface is usually difficult to control experimentally. Krishanu Ray adopted an improved method by using the same technique together with inert amphiphilic stearic acid layers in order to more accurately control the distance [80]. In this way, the distance between the fluorophore and surface island films can be tailored by varying the number of inert amphiphilic stearic acid layers to a resolution of ~2.5 nm. They also used silver island films as metallic materials and two long-chain nitrobenzoxadiazole derivatives (NBD-C16 and NBD-C18) as probes. As shown in Fig. 2, a maximum enhancement of 32 folds is accomplished in contact with the silver surface but the enhancement is reduced to 4 folds when the probe is 90 nm from the stearic acid layers. The maximum metal-enhanced fluorescence occurs when the probes are about 10 nm from the metallic structure. The findings suggest that silver nanostructures can be used to amplify the fluorescent signatures and increase the detection limits in cell imaging.

Considering the distance dependence, the use of fluorescence cellular imaging is extremely useful to the study of membrane proteins. The thickness of a cell membrane is typically about 7 nm, which is close to the optical distance for fluorescence enhancement. Therefore, fluorescence imaging of proteins on cell membranes is available without the worry of interference from signals inside the cell. It is known that membrane proteins play a key role in the physiology of living cells and carry out a number of important functions, for instance, energy metabolism, cell-cell interaction, or uptake of nutrients and ions [81]. Investigation of membrane proteins in the natural environment can provide more comprehensive results considering that many intricate molecular reactions take place in the highly dynamic and complex plasma membranes. Considering good biological compatibility and low background of surface enhanced cellular fluorescence imaging, this technology, which can probe proteins in the membranes of living cells, has great potential. By comparing the fluorescent intensities of the cell nuclei and membranes, the distance-dependent phenomenon can also be further verified [82]. Fig. 3 shows that the "nucleus labeled" cells can be imaged well by confocal microscopy on both the glass and silver island films. However, in contrast to the "membrane labeled" cells, the "nucleus labeled" cells on the metal show insignificant differences in both the intensity and lifetime from those on the glass. It is clear that the fluorophores in the cell membranes are localized within, but the fluorophores in the cell nuclei are beyond the region of metal-enhanced fluorescence. Thus, the metal can be used to improve the detection sensitivity of intrinsic fluorescent proteins and target molecules on cell surfaces when they are fluorescently labeled.

3.2. Surface patterns

Experiments have confirmed the importance of overlapping between the localized SP resonance energy of surface configuration and emission energy [83]. The type, shape, height, and density of the surface nanostructures determine the degree of enhancement. In order to explore the cause and mechanism, experiments have been conducted carefully often excluding other possible factors which may contribute to the enhancement such as reflection from the metallic nanostructures, emission from the metallic nanostructures themselves, increased absorption of light in photoluminescence enhancement, and quenching of defect emission. Although the exact mechanism is still debatable, it is generally agreed that the effects of metallic colloids interacting with fluorophores can be understood by the formation of metal interstitial sites. These interstitial sites, so-called "hot spots" or "hot junctions" in the nanostructures, consist of two or more coupled particles or nanostructured surfaces with closely spaced features, and there are highly concentrated EM fields associated with strong localized SP resonance [58].

Metallic colloids play an important role in surface-enhanced cellular fluorescence imaging. Although spraying silver or gold colloids onto a substrate leads to a high fluorescence signal from some local "hot spots", it is not easy to obtain a reliable, stable, and uniform signal with a wide dynamic range due to particle aggregation. Popular approaches to remedy the problems such as poor control of the particle aggregation states include surface immobilization [84], entrapment in stable matrices [85], and fabrication of complex surface structures (e.g. by means of microfabrication) [86,87]. For example, silver island films have been produced on glass by reduction of silver nitrate

[82]. These silver particles having lateral dimensions of 100 to 500 nm and height of 70 nm cover about 20% of the glass surface. They are protected by the terminal carboxylic acid thiolate ligands and so exist as metallic silver instead of oxide when cellular imaging is performed by confocal microscopy. The T-Lymphocytic cell lines are labeled by Alexa Fluor 680-dextran conjugates on the membranes or by YOYO (oxazole yellow dimer, benzo-1,3 oxazole in place of the benzo-1,3-thiazole, a common dye used in DNA analysis). The emission intensity from the silver island films is eight times brighter than that from glass. The overall fluorescence background due to cell autofluorescence is not affected appreciably by the silver island films but the emission lifetime of the adhered fluorophores on the cell surfaces is obviously shortened relative to that on glass.

Although the use of silver island films demonstrates the large potential of surface-enhanced cellular fluorescence imaging, the location of these hot spots on the silver island films is unpredictable, and the fluorescence intensity changes dramatically from one hot spot to another even on the same sample due to the irregular geometry. This is a major obstacle hampering practical applications and patterning the metallic surface with periodic corrugations may be a good alternative. We have fabricated patterned silver nanocap arrays by a simple coating technique using porous anodic alumina templates [32]. Silver is deposited directly on the porous anodic alumina substrate using direct-current magnetron sputtering. Since the porous anodic alumina templates have small protrusions along the surface of the pore wall, the silver nanocaps grow on the protrusions of the porous anodic alumina templates. As shown in Fig. 4(a), which depicts a representative SEM image of the sample surface, the silver nanocaps cover the alumina protrusions and a periodic hexagonal arrangement can be observed. The structures have a uniform size ($D = 50 \pm 5$ nm) due to the similar shape of the alumina protrusions and

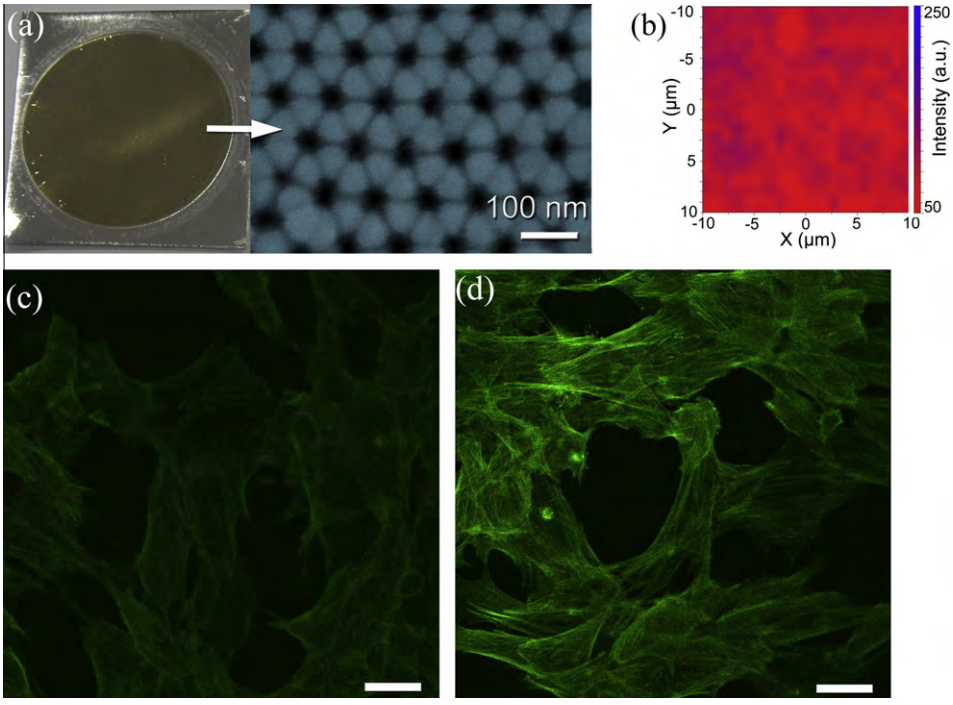

Fig. 4. (a) SEM image acquired from the patterned silver nanocap arrays. The inset in (a) shows large-area patterned silver nanocap arrays with a size exceeding 3 cm^2. (b) Surface-enhanced Raman map of a 20.0 × 20.0 μm^2 area of the patterned silver nanocap arrays. The map is obtained from the integrated intensity of the 612 ± 10 cm^{-1} band of 10^{-5} M rhodamine 6G adsorbed on the substrate. Representative confocal images of AG1522 cells labeled with P-FITC adhered to the cytoskeleton protein f-actin on the (c) glass slide and (d) patterned silver nanocap arrays excited by the 488 nm laser line. The scale bar is 20 μm. Reprinted with permission from [32]. Copyright 2010 American Chemical Society.

same sputtering time. Ortho-, meta-, and para-cap gaps can be observed and the ortho-cap gap is less than 10 nm. The size of each protuberance and inter-particle gap are controlled to around 100 nm and less than 10 nm respectively, which are necessary for big fluorescence enhancement. The homogeneity of the patterned silver nanocap arrays is evaluated by 2D point-by-point surface-enhanced Raman mapping of rhodamine 6G molecules and the results are exhibited in Fig. 4(b). The relative surface-enhanced Raman mapping peak intensity of the collection spots has a narrow range, and the spot-to-spot relative standard deviation is 5%. The data indicate that the substrate homogeneity is quite good and strict control of the preparation conditions can ensure good reproducibility among different batches. Ag1522, a normal human fibroblast culture derived from foreskins of 3-day-old male, and Chinese hamster ovary cells are labeled by phalloidin-fluorescein isothiocyanate on the cytoskeletons and the fluorescence signals from the fluorophores bound to the cell cytoskeletons on the patterned silver nanocap arrays are enhanced by 8 folds compared to those on glass used in conventional imaging, as illustrated in Fig. 4(c) and (d). In addition to the intensity enhancement, the photostability is improved dramatically. Thus the use of patterned silver nanocap arrays is a good means to improve the sensitivity and stability in cellular fluorescence imaging.

4. Nanostructured surfaces with evenly distributed plasmonic fields compatible with enhanced cellular fluorescence imaging

The practical success of enhanced cellular fluorescence imaging depends on the production of sub-wavelength nanostructures with evenly distributed plasmonic fields that can yield a high average enhancement factor. A properly designed substrate has many advantages over glass slides, but in spite of extensive research to produce a highly ordered metallic structure and develop different methods to micro-pattern metallic surfaces, nano-scale fabrication with good tunability is still challenging. The common techniques/materials and their potential are described and compared in this section.

4.1. Nanoparticle superlattice coatings

As new synthetic techniques are developed to produce metallic nanoparticles with a narrow size distribution, new fundamental questions akin to nanoparticle assembly into ordered arrays or nanoparticle superlattices have been raised [88]. If a nanoparticle is viewed as an "artificial atom," then a superlattice of nanoparticles is an "artificial solid" and there are several examples of metallic nanoparticle-based assemblies [89–92]. Nanoparticle superlattices can be obtained by slowly evaporating the solvent, which contains the monodispersed nanoparticles. The spacing between nanoparticles in the solids can be adjusted by modifying the capping materials such as alkanethiols with variable chain lengths.

Our group has recently fabricated passivated silver nanocrystals in bulk quantities *via* a conventional hydro-thermal method which provides a convenient nanotechnique to assemble noble metals with the superlattice structure [93]. The hydro-thermal method is based on the general phase transfer and separation mechanism occurring at the interfaces of the liquid, solid, and solution phases during synthesis. Fig. 5 depicts the bright-field transmission electron micrographs and corresponding electron diffraction patterns. The near-complete monolayer silver nanocrystals with a relatively narrow particle size distribution (5.0 ± 0.3 nm) can be clearly observed. Using as-grown passivated silver nanocrystals as the building blocks in conjunction with self-assembly, superlattice materials with controllable size and shape can be synthesized. The core size of the particles can be adjusted by temperature. The alkyl chains absorbed on the surface of the silver nanocrystals also provide interparticle bonding, which enhances the structural stability and maximum temperature the materials can withstand. By controlling the length of the alkyl chains (substituting with another fatty acid and sodium stearate for linoleic acid and sodium linoleate), the gap between two coupled silver nanocrystals can be tailored thus giving rise to the tunable properties. The silver nanocrystal superlattice can serve as a universal functional coating for molecular sensing in surface-enhanced Raman spectroscopy [94]. This coating exhibits a high Raman signal enhancement factor due to a very high density of both silver nanoparticles ($\sim 1.8 \times 10^{12}\,\mathrm{cm}^{-2}$) and hot junctions ($\sim 5.4 \times 10^{12}\,\mathrm{cm}^{-2}$). It is believed that this

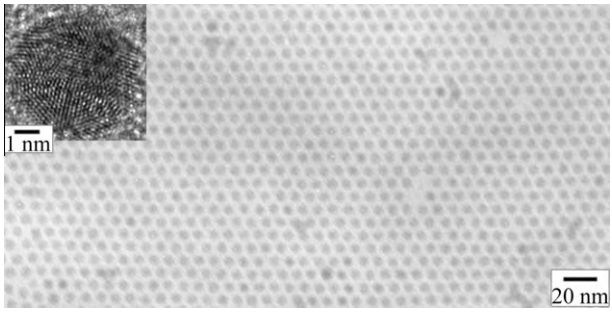

Fig. 5. Bright-field transmission electron micrographs of a self-assembled monolayer of silver nanocrystal superlattice. The inset shows the high-resolution image of a typical silver nanocrystal. Reprinted with permission from [94]. Copyright 2006 American Institute of Physics.

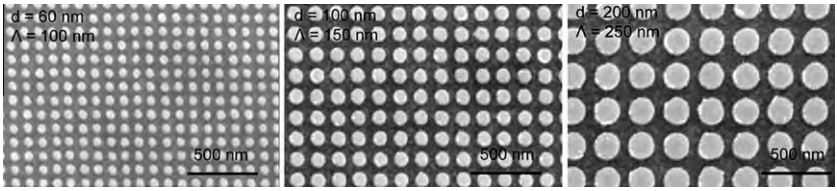

Fig. 6. SEM images of three gold nanodisks with diameters of 60, 100, and 200 nm and gratings of 100, 150, and 250 nm, respectively. The heights of all nanodisks are 50 nm. Reprinted with permission from [96]. Copyright 2008 American Chemical Society.

nanoparticle superlattice coating constitutes a potential nanostructured surface with evenly distributed plasmonic fields that can enhance cellular fluorescence imaging, but more work is needed prior to large-scale adoption.

4.2. Lithographically-based substrates

Lithography is a common method to produce materials with a feature size of less than 100 nm. A typical lithographic system consists of the following components [95]: (1) a mask that contains the patterns to be transferred and tools to ensure precise pattern transfer, (2) an energy source (for example, a light source) to transfer the pattern from the mask to substrate, (3) a photoresist or resist to record the patterns on the substrate during exposure, and (4) procedures for reliable detection of pattern defects, which clearly become more challenging as the critical dimensions diminish. However, most optical lithographic techniques do not have sufficient resolution to produce small enough and tightly spaced plasmonic geometries. In comparison, electron beam lithography, which utilizes electrons in lieu of photons has been successfully used to produce sub-10 nm structures due to the better spatial resolution and larger depth of focus compared to conventional photolithography. Yu, et al. have performed a systematic study on surface-enhanced spectroscopy of gold nanohole arrays with diameters between 40 and 520 nm and edge-to-edge distances between 60 and 120 nm. The materials are fabricated by electron beam lithography and the results are compared to those obtained from gold nanodisk arrays with comparable geometric parameters [96]. Fig. 6 shows the SEM images of three gold nanodisks with diameters of 60, 100, and 200 nm and gratings with sizes of 100, 150, and 250 nm. The height of the nanodisks is 50 nm. The tunable optical properties originate from the difference in the localized SP resonance modes that are most efficiently excited in the nanohole and nanodisk arrays. The large tolerance on dimensions and the empty space confined by the nanoholes suggest that they can be used as a functional component in enhanced cellular fluorescence imaging.

Although electron beam lithography offers high resolution and can delineate extraordinarily fine patterns, it has a small sample throughput and so alternative techniques have been proposed. One example is nanosphere lithography which has many desirable characteristics as a laboratory-scale nanofabrication tool [97]. Nanosphere lithography is relatively inexpensive while offering parallel processing and high throughput and can produce 2D periodic arrays of many types of nanoparticles on a variety of substrates. Nanosphere lithography has been demonstrated to produce size-tunable periodic silver nanoparticle arrays that are plasmonically active nanostructures by selecting the appropriate nanosphere diameter and/or thickness [98–101] (Fig. 7).

4.3. Alumina-templated surface

In comparison with conventional lithographic techniques, the use of porous anodic alumina membranes as templates to fabricate plasmonic nanostructured surfaces for enhanced cellular fluorescence imaging is promising considering the easy fabrication, excellent reproducibility, modest cost, and large area production capability. Moreover, the technique has the following advantages: (1) the ability to optimize periodic plasmonic geometries and tune the "hot junction" in the sub-10 nm regime and

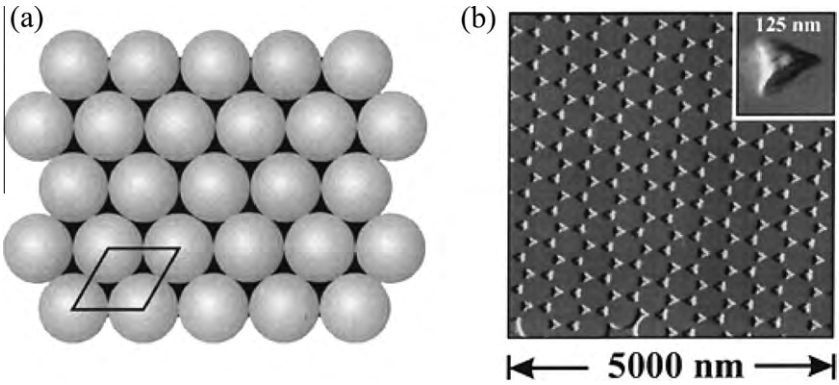

Fig. 7. (a) Schematic illustration and (b) representative atomic force microscopy image of the single layer periodic particle array. The ambient contact mode atomic force microscopy image is captured from a single layer periodic particle array fabricated with $D = 542$ nm nanospheres and $d_m = 48$ nm thermally evaporated silver after 3 min sonication in methylene chloride. Reprinted with permission from [101]. Copyright 2001 American Chemical Society.

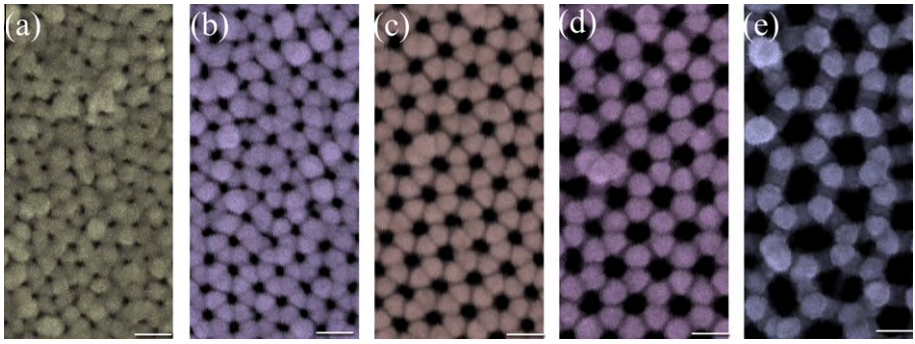

Fig. 8. A series of SEM images acquired from the silver coated porous anodic alumina membranes formed under different constant direct-current voltages: (a) 20, (b) 30, (c) 40, (d) 50, and (e) 60 V, respectively. Scale bar: 100 nm. The silver sputtering time is 10 min. Reprinted with permission from [115]. Copyright 2009 American Institute of Physics.

(2) creation of long-range uniform plasmonic structures with cm dimensions. Porous anodic alumina membranes are formed due to the self-organizing property when an Al foil is used as an anode in an electrolytic cell. The resulting densely-packed nanopore array has diameters varying from several to hundreds of nanometers. The formation mechanism and self-organization properties have been studied and several models have been proposed to describe the evolution of the nanopores in the porous anodic alumina membranes [102–104]. From both the commercial and technical viewpoints, porous anodic alumina membranes with highly ordered nanopore arrays have many advantages and so efforts have been made to improve the pore patterns [105,106]. In addition to experimental conditions such as temperature, electrolyte concentration, and applied anodic voltage, different pre-texturing processes have been developed to initiate pore growth on the Al surface and enhance the order of the resulting patterns [107,108]. With careful optimization, a defect free region with an area of several square centimeters has been produced [106]. In fact, the use of porous anodic alumina membranes as templates has been studied extensively and they can be used to fabricate various types of low-dimensional nanostructures including nanodots [109], nanowires [110], and nanotubes [111]. Metals and semiconductor materials can also be embedded into the porous anodic alumina membranes by electrodeposition [112], chemical vapor deposition [113], and other physical or chemical methods.

A convenient nanotechnique has recently been reported to fabricate highly ordered hemispherical silver nanocap arrays templated by porous anodic alumina membranes as optical nanoantenna systems to support localized SP resonance at optical frequencies [114]. On account of the periodic hexagonal arrangement and precise gap control between the nanostructures in the sub-10 nm regime, a high density of "hot spots" can be produced to yield enhanced fluorescence [115]. As shown in Fig. 8, the surface structure can further be modified to optimize the enhancement factor by porous anodic alumina fabrication and silver deposition. The use of porous anodic alumina membranes as templates to produce optical nanoantennae is especially promising considering the flexibility when spectrally tuning the SP resonance and controlling the ratio of the scattering to absorption cross sections.

5. Major applications of surfaced-enhanced cellular fluorescence imaging

Surface-enhanced cellular fluorescence imaging is one of the most exciting surface-sensitive methods to study and analyze biomolecular interactions. It offers many advantages such as surface-sensitive response, label-free detection, real-time measurement capability, possibility of single-molecule detection, and super-resolution imaging [6,116,117]. Several interesting and inspiring applications are described in this section to illustrate the broad scope and impact of this technology.

5.1. Single molecule detection (SMD)

SMD is usually performed on surface-immobilized molecules with a diffraction-limited volume using confocal optics to suppress the background from the sample and instrument. In order to detect a single molecule, the fluorescence sensitivity must be increased by modifying the spectral properties of the probes, enhancing the detection efficiency of the instrument, and amplification methods. Surface-enhanced fluorescence cellular imaging can deliver such performance because the amplification of fluorescence is a nanoscale phenomenon with a sharp distance dependence, which is ideally suited for the monitoring of bio-recognition reactions. By accurately controlling the distance between the cell and metal, the fluorescence signal from the targeted area within the enhancing distance can be amplified while others remain the same or are quenched.

With regard to SMD in whole blood, the autofluorescence is problematic but it is possible to increase the signal-to-noise ratio by reducing the sample volume. A recent experiment was carried out on metallic nanostructured surfaces to detect single surface bound Cy5-labeled DNA oligomers in diluted blood serum [118]. It is commonly accepted that in fluorescent signal-molecular detection, the probed volume has to be about 1 fL in order not to overwhelm the signal from background emission and Raman scattering [119]. By enhancing the fluorescence signal in the presence of metallic nanostructures, the signal-to-noise ratio of Cy5 in serum is increased four to ten times in the focused

mode, making it possible to access a volume of 1 pL in which the background from undiluted blood serum is approximately equal to 2700 Cy5 molecules. It implies the possibility of detecting a single fluorophore in a larger focused volume in a sample with a high background. The results also suggest the possibility of clinical assays based on SMD in blood serum and perhaps whole blood. The increased signal-to-noise ratio near the metallic nanostructure can obviate the need for the diffraction-limited volume and enhance the ability to conduct *in situ* single molecule detection.

These high backgrounds appear to preclude the possibility of SMD of Cy5 molecules. However, the signal-to-noise ratio (SNR) in high background samples can be increased dramatically by reducing the volume. Single surfacebound Cy5-labeled DNA (Cy5-DNA) oligomers can be detected from the diluted blood serum with an SNR near 40. We have also examined freely diffusing Cy5-DNA in blood serum. Single Cy5-DNA molecules can be detected even from the undiluted serum. We have further investigated the SNR on silver island films and found that the fluorescence signal is greatly enhanced in the presence of metallic nanostructures showing a larger SNR in the application tested. These results suggest the possibility of clinical assays based on SMD in blood serum and possibly whole blood. The increased SNR near the metallic nanostructure can probably overcome the need for diffraction-limited volumes and enhance our ability to perform *in situ* SMD.

Intrinsic emission from the DNA bases is extremely weak and it is possible to increase the intrinsic base emission from DNA by adopting metallic nanostructures. To avoid complex amplification steps, pare costs, and accomplish detection of a single DNA molecule or nucleotide during sequencing, the sensitivity of DNA detection must be increased. Metallic surfaces can increase the sensitivity of fluorescence and brightness of the single labeled oligonucleotides because of coupling between the fluorophores and SPs on the metallic surface. The effects of porous silver membranes on fluorescently labeled DNA oligomers have been studied and a 100 fold enhancement in the fluorescence emission has been observed from a porous silver substrate [120]. The porous silver membranes have a large specific surface area available for the fluorescent probes giving rise to big emission amplification. Additionally, the metallic substrates provide the flow-through format for both single molecules and many molecular DNA assays and it is possible to increase the intrinsic emission, which is extremely weak in general. There are extensive ongoing efforts to achieve high-throughput and low-cost DNA sequencing. One of the methods is to employ an exonuclease to sequentially remove DNA bases from a single strand of DNA [121].

Metal probes have recently been used to bind to cell surfaces to monitor the emission intensity or lifetime. The emission signals from the metal probes can be isolated and counted from the cell images, especially lifetime images [122]. An approach to use these metal probes to quantify the number of target molecules on the cell surfaces in single cell images has been proposed [123]. In this study, Cy5-avidin conjugates are covalently bound onto 20 nm silver particles as the molecular imaging reagent [124]. Relative to other fluorescence applications, the avidin-metal complexes on the cell surface display stronger emission signal, shorter lifetime, and better photostability [125]. When the cell surfaces are biotinylated at a low level, the avidin-metal complexes bound to the cell surfaces can be identified as isolated emission spots distinct from cellular autofluorescence. A way to quantify the amount of target molecules on the cell surfaces by monitoring the cell intensity and lifetime images at the single cell level has also been suggested. As the lifetime over the entire cell images is significantly altered by the amount of biotin-sites on the cell surface, a quantitative regression curve between the amount of avidin-metal complex on the cell surface and the emission lifetime over the entire cell image can be obtained. The regression curve is used to infer the number of target molecules on the cell surfaces and the relative error is about 30%. Because a larger avidin-metal complex amount on the cell surface may make it difficult to count the closely spaced probes, the regression curve may not be accurate because the linear relationship is simply by approximation. Hence, further improvement is required. In spite of imperfections in the method, it is indeed progress for SMD by providing an idea to detect or count molecules in cell membrane with high accuracy. By modifying the dying conjugates, adjusting experimental conditions, and improving the model for counting, better results may be possible [126,127].

In spite of exciting progress, more work is still needed to conduct SMD on metallic surfaces in practice, for example, detection of single miRNA in lung cancer cells [128], detection of fluorescence green proteins [129], and SMD of biological macromolecules [130]. Nonetheless, results published so far demonstrate the potential of plasmonic nanostructured surfaces. In conclusion, SMD of a fluorophore

near silver particles allows direct observation of various fluorescence characteristics of individual molecules and imparts detailed information about the emission from a single fluorophore and its interaction with interfaces. Further development of fluorophore-metal interactions for SMD requires defined structures and ordered nanostructures with evenly distributed plasmonic fields may further improve the detection precision.

5.2. Long-term imaging with high resolution

Current research activities focus on the improvement of the spatial resolution in order to realize video-rate imaging of living cells with molecular resolution. The use of a silver coated plain glass as gratings in high-resolution fluorescence microscopy has been demonstrated using standard commercial optical fluorescence microscopes without additional accessories [131]. Silver coated gratings with the tailored duty ratio and depth and periodical pitch of 400 nm are designed and implemented. The grating structures are fabricated on quartz by dual-beam interference followed by silver sputter coating. The gratings with the designed depth and duty ratio are investigated experimentally and theoretically to identify the optimal conditions for the highest fluorescence enhancement. Based on the reflectivity curves, the best SP resonance response, a minimum reflectivity of 1%, is obtained on gratings with a duty ratio of 0.43 (0.50 after coating) at a depth of 20 nm. The interpretation these results is consistent with the explanation produced in a recent study on grating-assisted prism-coupled SP resonance by Giannattasio et al., in which the profile of the grating corrugation is expressed in terms of Fourier expansion [132]. At each optimum duty ratio, the SP coupling and fluorescence enhancement for different grating depths are investigated and a grating with a depth of 20 nm is found to yield

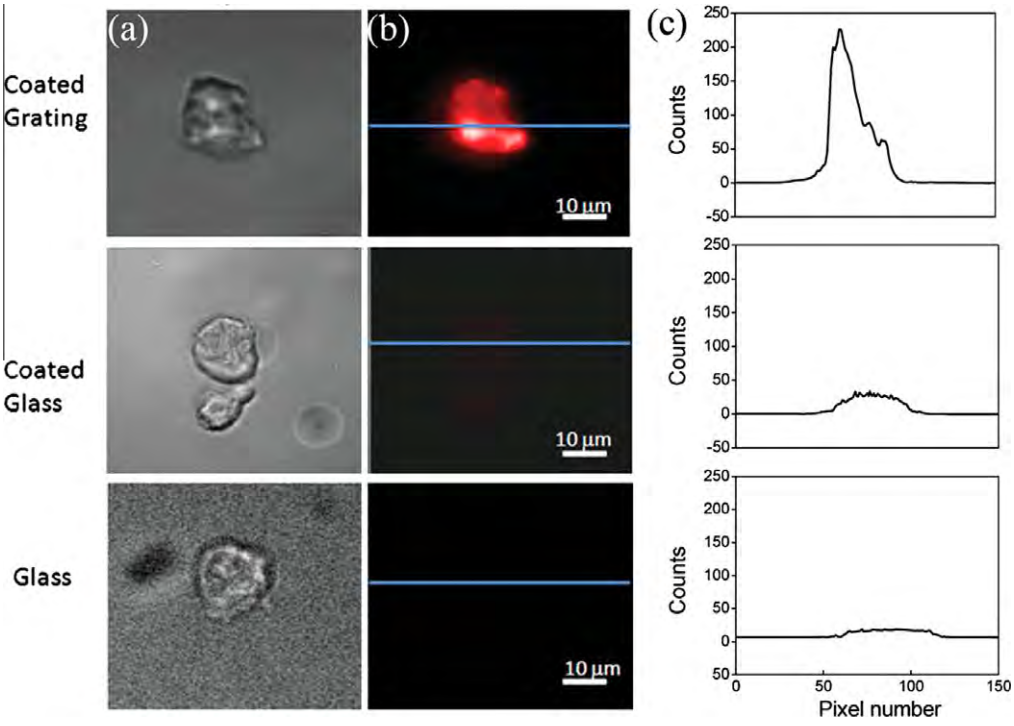

Fig. 9. Microscopic observations of Cy5-labeled cells on different substrates: (a) Bright field images, (b) Fluorescence images under same intensity scale, and (c) Fluorescence line profiles taken from the images in (b). Reprinted with permission from [131]. Copyright 2010 John Wiley & Sons, Inc.

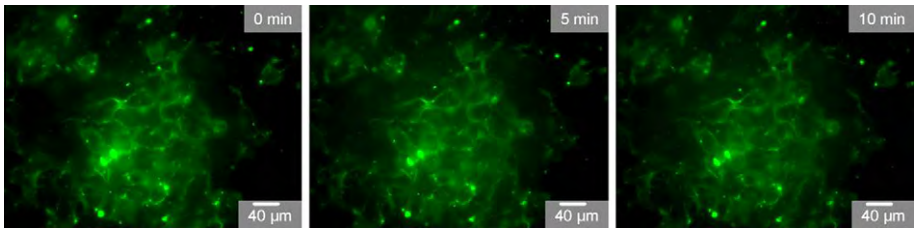

Fig. 10. Fluorescence image of the same area of labelled COS-7 cells (using TAT functionalized Au-fluorescein nanoparticle) under continuous blue excitation for 0, 5 and 10 min. The fluorescence does not bleach, indicating the long term fluorescence stability of the plasmonic fluorescent gold nanoparticle. Reprinted with permission from [146]. Copyright 2009 American Chemical Society.

higher fluorescence enhancement than those with depths of 10 and 30 nm. Their potential in cell imaging is explored by observing the transfected GFP cells binding with the antibody–Cy5 conjugation on a commercial fluorescence microscope without hardware modification. As shown in Fig. 9, the fluorescence image from the silver-coated grating is much clearer than that from the flat silver and bare glass surfaces on the same fluorescence intensity scale. The profiles across the cells in Fig. 9(c) show the enhancement effect of the coated grating substrates. The background subtracted fluorescence intensities observed from the three substrates are about 240, 30, and 10 counts per unit pixel, respectively, demonstrating the potential in high-resolution fluorescence microscopy.

Besides the use of metal surfaces as gratings for long-term imaging with high resolution, another trend is to fabricate plasmonic-fluorescent composite nanoparticles as alternative molecular imaging probes [133–140], for example, Au/Ag nanoparticle-organic fluorophore-based and Au/Ag nanoparticle-quantum dot composites. The basic idea is to create metal-fluorophore complexes in which the metal particle increases the brightness of the bound fluorophores. This can be accomplished by coating metal particles with fluorophores. The theoretical prediction is that fluorophores in the metal shells can be 100-fold brighter than isolated ones, even after considering the transfer efficiency of incident light into the shell and radiation out of the shell [141,142]. In order to minimize fluorescence quenching, a separation distance of more than 5 nm should be maintained between the Au/Ag particle and fluorophore/quantum dot [143–145]. This requirement increases the overall diameter of the composite particle to >50 nm, which often decreases the water solubility and cellular entry thereby limiting cell labeling applications. Recently, smaller diameter (20–30 nm) plasmonic-fluorescent nanoparticles composed of Au/Ag nanoparticles and fluorescein have been prepared [146]. These particles are composed of 3–6 nm diameter Au/Ag cores and fluorescein-incorporated polymeric shells. They have bright, stable, and tunable properties and can be made into functional nanoprobes. Fig. 10 illustrates an example of using TAT functionalized gold nanoparticles to label COS-7 cells. The positive surface charge and multiple TAT functionality on each particle induce strong interactions with cell membranes and so a nanomolar concentration of the particles is sufficient to produce labeling effects under a fluorescence microscope. The probe stability has been investigated and fluorescence images acquired from the same area of labeled COS-7 cells under continuous blue excitation for 0, 5, and 10 min have been compared. The fluorescence does not bleach and so the long term fluorescence stability of plasmonic fluorescent gold nanoparticles is verified. This method is similar to imaging methods with quantum dots. Since silver films are expected to have low cytotoxicity than QDs and it is possible to obtain long-term dynamic images using these novel fluorescent probes.

6. Conclusion and future challenges

While researching wireless telegraphy in 1917, Jonathan Zenneck analyzed the propagation of EM waves over extended metallic surfaces [147] and 50 years later, SPs were recognized [148]. At that time, probably few people would have expected the tremendous interest in SPs today, spanning quantum optics and data storage to spectroscopy and medicine. In fact, even in the early 1960s, SPs were

mainly of academic interest until researchers realized that the intense EM fields associated with SPs generated in the vicinity of a metal interface could be used to sense small dielectric-constant changes associated with adsorbed molecules on the surface. To researchers working in optics, one of the most attractive aspects of SPs is the way in which they concentrate and channel light using these subwavelength structures. Concentrating light in this way leads to an electric field enhancement that can be used to manipulate light–matter interactions and boost non-linear phenomena. The enhanced localized EM field near the metallic surface gives birth to surface-enhanced Raman scattering [149] and modern nanofabrication and characterization techniques have made it possible to structure metallic surfaces to steer and control the flow of SPs and to map the flow with unprecedented details [150–153]. A number of physicochemical effects related to the behavior of fluorophores in complex dielectric and metal environments have been brought into focus by the emergence of the field of plasmonics. The interactions between fluorophores and plasmons suggest that the novel optical absorption and scattering properties of metallic nanostructures can be used to control the decay rates, location, and direction of fluorophore emission.

Applications of metal-enhanced fluorescence continue to proliferate covering exciting topics in biological, medical, and physical sciences thanks to the unique surface sensitivity, label-free detection, and real-time measurement capability. However, although substantial progress has been made on the mechanism of fluorescence enhancement, there are still many challenges and some important ones are discussed here.

(1) *Distance measurements:* Distance measurements in the range from 10 to 200 nm offer important insights to the design of the optimal surface configurations in enhanced cellular fluorescence imaging. Fluorescence resonance energy transfer and certain electron paramagnetic resonance-based experiments can be used to measure the distance in the nanometer range without restriction by the size of the biomolecule [154]. Distances ranging from macroscopic to about $\lambda/2$, typically 300 nm, can be determined by confocal, multiphoton, and/or laser scanning methods [155,156]. It should be noted that the distance between the fluorophore and metal is not measured in most experiments and there have only been recent attempts to identify the optimal distance. Additional studies are needed to determine the range of distances that can be used in surface-enhanced cellular fluorescence imaging.
(2) *Surface fabrication:* It is challenging to prepare uniform nanosurfaces using existing techniques. Although a nanostructured surface with evenly distributed plasmonic fields has been produced, there is room for further optimization. Reproducible aggregation of solution-phase nanoparticles is hard to achieve and fabricating periodic structures with an interparticle gap of less than 2 nm (necessary for intense enhancement) is also challenging. Moreover, surface defects are inevitable due to experimental randomness and environmental factors. Improved parameters and reaction conditions as well as new fabricating methods to reduce defects must be explored.

All in all, we have reviewed succinctly recent advances pertaining to surface-enhanced cellular fluorescence imaging and discussed the associated mechanisms and future challenges. The technique plays an important role in the study of intracellular processes at the single-molecular level. It is particularly useful to high-resolution cellular imaging, long-term *in vivo* observation of cell trafficking, tumor targeting, and diagnostics. Although research in surface-enhanced cellular fluorescence imaging is still in the early stage, much progress is expected in the near future due to the tremendous potential and versatile applications.

Acknowledgements

This work was jointly supported by the National Natural Science Foundation of China under Grant No. 51071045, the Program for New Century Excellent Talents in University of Ministry of Eduction of China, Southeast University, Hong Kong Research Grants Council (RGC) General Research Funds (GRF) No. CityU 112510, and City University of Hong Kong Research Grant No. 9360110.

References

[1] J.F.W. Herschel, On a case of superficial colour presented by a homogeneous liquid internally colourless, Phil. Trans. Roy. Soc. Lond. 135 (1845) 143–145.
[2] G.G. Stokes, On the change of refrangibility of light, Phil. Trans. Roy. Soc. Lond. 142 (1852) 463–562.
[3] P. Kask, K. Palo, D. Ullmann, K. Gall, Fluorescence-intensity distribution analysis and its application in biomolecular detection technology, P. Natl. Acad. Sci U. S. A. 96 (1999) 13756–13761.
[4] B. Liedberg, C. Nylander, I. Lundström, Biosensing with surface plasmon resonance—how it all started, Biosens. Bioelectron. 10 (1995) i–ix.
[5] J. Homola, S.S. Yee, G. Gauglitzb, Surface plasmon resonance sensors: review, Sensor. Actuat. B – Chem. 54 (1999) 3–15.
[6] O. Stranik, H.M. McEvoy, C. McDonagh, B.D. MacCraith, Plasmonic enhancement of fluorescence for sensor applications, Sensor. Actuat. B-Chem. 107 (2005) 148–153.
[7] P.S. Langendijk, F. Schut, G.J. Jansen, G.C. Raangs, G.R. Kamphuis, M.H.F. Wilknson, G.W. Welling, Quantitative fluorescence in situ hybridization of *bifidobacterium* spp. with genus-specific 16S rRNA-targeted probes and its application in fecal samples, Appl. Environ. Microb. (1995) 3069–3075.
[8] W.F. Patton, A thousand points of light: the application of fluorescence detection technologies to two-dimensional gel electrophoresis and proteomics, Electrophoresis 21 (2000) 1123–1144.
[9] K. Aslan, Y. Zhang, S. Hibbs, L. Baillie, M.J.R. Previtea, C.D. Geddes, Microwave-accelerated metal-enhanced fluorescence. application to detection of genomic and exosporium anthrax DNA in <30 seconds, Analyst 132 (2007) 1130–1138.
[10] L.A.D. Zucchi, V.F.N. Filho, H.S. Neto, Application of X-ray fluorescence to determination of metals in commercial tablets containing digoxin, J. Trace Microprobe. T. 20 (2002) 141–149.
[11] S. Tyagi, F.R. Kramer, Molecular beacons: probes that fluoresce upon hybridization, Nat. Biotechnol. 14 (1996) 303–308.
[12] S. Tyagi, D.P. Bratu, F.R. Kramer, Multicolor molecular beacons for allele discrimination, Nat. Biotechnol. 16 (1998) 49–53.
[13] F.S. Wouters, P.J. Verveer, P.I.H. Bastiaens, Imaging biochemistry inside cells, Trends Cell. Biol. 11 (2001) 203–211.
[14] P.J. Tadrous, Methods for imaging the structure and function of living tissues and cells: 2. Fluorescence lifetime imaging, J. Pathol. 191 (2000) 229–234.
[15] J.A. Levitt, D.R. Matthews, S.M. Ameer-Beg, K. Suhling, Fluorescence lifetime and polarization-resolved imaging in cell biology, Curr. Opin. Biotech. 20 (2009) 28–36.
[16] A.N. Asanov, W.W. Wilson, P.B. Oldham, Regenerable biosensor platform: a total internal reflection fluorescence cell with electrochemical control, Anal. Chem. 70 (1998) 1156–1163.
[17] H.P. Lehr, M. Reimann, A. Brandenburg, G. Sulz, H. Klapproth, Real-time detection of nucleic acid interactions by total internal reflection fluorescence, Anal. Chem. 75 (2003) 2414–2420.
[18] L.G. Kostrikis, S. Tyagi, M.M. Mhlanga, D.D. Ho, F.R. Kramer, Spectral genotyping of human alleles, Science 279 (1998) 1228–1229.
[19] Kadir Aslan, C.D. Geddes, Microwave-accelerated metal-enhanced fluorescence (MAMEF): application to ultra fast and sensitive clinical assays, J. Fluoresc. 16 (2006) 3–8.
[20] E. Phizicky, P.I.H. Bastiaens, H. Zhu, M. Snyder, S. Fields, Protein analysis on a proteomic scale, Nature 422 (2003) 208215.
[21] M.H. Chowdhury, K. Ray, M.L. Johnson, S.K. Gray, J. Pond, J.R. Lakowicz, On the feasibility of using the intrinsic fluorescence of nucleotides for DNA sequencing, J. Phys. Chem. C 114 (2010) 7448–7461.
[22] A. Miyawaki, A. Sawano, T. Kogure, Lighting up cells: labelling proteins with fluorophores, Nat. Cell. Biol. Suppl. (2003) S1–S7.
[23] J.L. Kovar, M.A. Simpson, A. Schutz-Geschwender, D.M. Olive, A systematic approach to the development of fluorescent contrast agents for optical imaging of mouse cancer models, Anal. Biochem. 367 (2007) 1–12.
[24] T. Suzuki, T. Matsuzaki, H. Hagiwara, T. Aoki, K. Takata, Recent advances in fluorescent labeling techniques for fluorescence microscopy, Acta. Histochem. Cytochem. 40 (2007) 131–137.
[25] J.R. Lakowicz, Radiative decay engineering: biophysical and biomedical applications, Anal. Biochem. 298 (2001) 1–24.
[26] M. Fernández-Suárez, A.Y. Ting, Fluorescent probes for super resolution imaging in living cells, Nat. Rev. Mol. Cell Biol 9 (2008) 929–943.
[27] P. Lang, K. Yeow, A. Nichols, A. Scheer, Cellular imaging in drug discovery, Nat. Rev. Drug. Discov. 5 (2006) 343–356.
[28] T. Nagano, T. Yoshimura, Bioimaging of nitric oxide, Chem. Rev. 102 (2002) 1235–1269.
[29] J.P. Knemeyer, D.P. Herten, M. Sauer, Detection and identification of single molecules in living cells using spectrally resolved fluorescence lifetime imaging microscopy, Anal. Chem. 75 (2003) 2147–2153.
[30] M. Monici, Cell and tissue autofluorescence research and diagnostic applications, Biotechnol. Annu. Rev. 11 (2005) 227–256.
[31] S.J. Rosenthal, A. Tomlinson, E.M. Adkins, S. Schroeter, S. Adams, L. Swafford, J. McBride, Y.Q. Wang, L.J. DeFelice, R.D. Blakely, Targeting cell surface receptors with ligand-conjugated nanocrystals, J. Am. Chem. Soc. 124 (2002) 4586–4594.
[32] T. Qiu, J. Jiang, W.J. Zhang, X.Z. Lang, X.Q. Yu, P.K. Chu, High-sensitivity and stable cellular fluorescence imaging by patterned silver nanocap arrays, ACS Appl. Mater. Interfaces 2 (2010) 2465–2470.
[33] W.L. Barnes, Fluorescence near interfaces: the role of photonic mode density, J. Mod. Opt. 45 (1998) 661–699.
[34] H. Metiu, Surface enhanced spectroscopy, Prog. Surf. Sci. 17 (1984) 153–320.
[35] K.H. Drexhage, Influence of a dielectric interface on fluorescence decay time, J. Lumin. 1–2 (1970) 693–701.
[36] B.N.J. Persson, Theory of the damping of excited molecules located above a metal surface, J. Phys. C 11 (1978) 4251–4269.
[37] K.L. Kelly, E. Coronado, L.L. Zhao, G.C. Schatz, The optical properties of metal nanoparticles: the influence of size shape and dielectric environment, J. Phys. Chem. B 107 (2003) 668–677.
[38] G. Chumanov, K. Sokolov, B.W. Gregory, T.M. Cotton, Colloidal metal films as a substrate for surface-enhanced spectroscopy, J. Phys. Chem. 99 (1995) 9466–9471.
[39] K. Sokolov, G. Chumanov, T.M. Cotton, Enhancement of molecular fluorescence near the surface of colloidal metal films, Anal. Chem. 70 (1998) 3898–3905.
[40] J.R. Lakowicz, K. Ray, M. Chowdhury, H. Szmacinski, Y. Fu, J. Zhang, K. Nowaczyk, Plasmon-controlled fluorescence. a new paradigm in fluorescence spectroscopy, Analyst 133 (2008) 1308–1346.

[41] R.R. Chance, A. Prock, R. Silbey, Lifetime of an emitting molecule near a partically reflecting surface, J. Chem. Phys. 60 (1974) 2744–2748.
[42] J. Gersten, A. Nitzan, Spectroscopic properties of molecules: interacting with small dielectric particles, J. Chem. Phys. 75 (1981) 1139–1152.
[43] R. Ruppin, Decay of an excited molecule near a small metal sphere, J. Chem. Phys. 76 (1982) 1681–1684.
[44] J. Kümmerlen, A. Leitner, H. Brunner, F.R. Aussenegg, A. Wokaun, Enhanced dye fluorescence over silver island films: analysis of the distance dependence, Mol. Phys. 80 (1993) 1031–1046.
[45] T. Qiu, X.L. Wu, G.G. Siu, P.K. Chu, Self-assembled growth and green emission of gold nanowhiskers, Appl. Phys. Lett. 87 (2005) 223115.
[46] R.R. Chance, A. Prock, R. Silbey, Molecular fluorescence and energy transfer near interfaces, Adv. Chem. Phys. 37 (1978) 1–65.
[47] G.W. Ford, W.H. Weberel, Ectromagnetic interactions of molecules with metal surfaces, Phys. Rep. 113 (1984) 195–287.
[48] M. Moskovits, Surface-enhanced spectroscopy, Rev. Mod. Phys. 57 (1985) 783–826.
[49] E. Fort, S. Grésillon, Surface enhanced fluorescence, J. Phys. D Appl. Phys. 41 (2008) 1–31.
[50] W.L. Barnes, A. Dereux, T.W. Ebbesen, Surface plasmon subwavelength optics, Nature 424 (2003) 824–830.
[51] J.R. Sambles, G.W. Bradbery, F.Z. Yang, Optical-excitation of surface-plasmons – an introduction, Contemp. Phys. 32 (1991) 173–183.
[52] B. Hecht, H. Bielefeldt, L. Novotny, Y. Inouye, D.W. Pohl, Local excitation, scattering, and interference of surface plasmons, Phys. Rev. Lett. 77 (1996) 1889–1892.
[53] H. Ditlbacher, J.R. Krenn, N. Felidj, B. Lamprecht, G. Schider, M. Salerno, A. Leitner, F.R. Aussenegg, Fluorescence imaging of surface plasmon fields, Appl. Phys. Lett. 80 (2002) 404–406.
[54] R.H. Ritchie, E.T. Arakawa, J.J. Cowan, R.N. Hamm, Surface-plasmon resonance effect in grating diffraction, Phys. Rev. Lett. 21 (1968) 1530–1533.
[55] E. Kretschmann, H. Raether, Radiative decay of nonradiative surface plasmons excited by light, Z. Naturforsch. A 23 (1968) 2135–2136.
[56] A. Otto, Exitation of nonradiative surface plasma waves in silver by the method of frustrated total reflection, Z. Phys. 216 (1968) 398–410.
[57] H. Raether, Surface Plasmons, Springer, Berlin, 1988.
[58] E. Hutter, J.H. Fendler, Exploitation of localized surface plasmon resonance, Adv. Mater. 16 (2004) 1685–1706.
[59] J.J. Bowman, T.B.A. Senior, P.L.E. Uslenghi, Electromagnetic and Acoustic Scattering by Simple Shapes, Hemisphere Publishing Corp, New York, 1987.
[60] H. Okamoto, K. Imura, Near-field optical imaging of enhanced electric fields and plasmon waves in metal nanostructures, Prog. Surf. Sci. 84 (2009) 199–229.
[61] J.R. Lakowicz, Y. Shen, S. D'Auria, J. Malicka, J. Fang, Z. Gryczynski, I. Gryczynski, Radiative decay engineering: 2. Effects of silver island films on fluorescence intensity, lifetimes, and resonance energy transfer, Anal. Biochem. 301 (2002) 261–277.
[62] J.R. Lakowicz, J. Malicka, I. Gryczynski, Z. Gryczynski, C.D. Geddes, Radiative decay engineering the role of photonic mode density in biotechnology, J. Phys. D Appl. Phys. 36 (2003) R240–R249.
[63] J.R. Lakowicz, Radiative decay engineering: 3. Surface plasmon-coupled directional emission, Anal. Biochem. 324 (2004) 153–169.
[64] I. Gryczynski, J. Malicka, Z. Gryczynski, J.R. Lakowicz, Radiative decay engineering: 4. Experimental studies of surface plasmon-coupled directional emission, Anal. Biochem. 324 (2004) 170–182.
[65] J.R. Lakowicz, Radiative decay engineering: 5. Metal-enhanced fluorescence and plasmon emission, Anal. Biochem. 337 (2005) 171–194.
[66] J.R. Lakowicz, Principles of Fluorescence Spectroscopy, Springer, New York, 2006.
[67] D. Toptygin, Effects of the solvent refractive index and its dispersion on the radiative decay rate and extinction coefficient of a fluorescent solute, J. Fluoresc. 13 (2003) 201–219.
[68] J.R. Lakowicz, C.D. Geddes, I. Gryczynski, J. Malicka, Z. Gryczynski, K. Aslan, J. Lukomska, E. Matveeva, J. Zhang, R. Badugu, J. Huang, Advances in surface-enhanced fluorescence, J. Fluoresc. 14 (2004) 425–441.
[69] I. Pockrand, A. Brillante, D. Möbius, Nonradiative decay of excited molecules near a metal surface, Chem. Phys. Lett. 69 (1980) 499–504.
[70] H. Knobloch, H. Brunner, A. Leitner, F. Aussenegg, W. Knoll, Probing the evanescent field of propagating plasmon surface polaritons by fluorescence and Raman spectroscopies, J. Chem. Phys. 98 (1993) 10093–10095.
[71] R.M. Amos, W.L. Barnes, Modification of the spontaneous emission rate of Eu^{3+} ions close to a thin metal mirror, Phys. Rev. B 55 (1997) 7249–7254.
[72] A. Ulman, An Introduction to Ultrathin Organic Films: From Langmuir–Blodgett to Self-Assembly, Academic Press, Boston, 1991.
[73] P.A. Antunes, C.J.L. Constantino, R.F. Aroca, Langmuir and Langmuir–Blodgett films of perylene tetracarboxylic derivatives with varying alkyl chain length film packing and surface-enhanced fluorescence studies, Langmuir 17 (2001) 2958–2964.
[74] K.H. Drexhage, Interaction of light with monomolecular dye layers, Prog. Opt. 12 (1974) 163–232.
[75] D.H. Waldeck, A.P. Alivisatos, C.B. Harris, Nanradiative damping of molecular electronic excited states by metal surfaces, Surf. Sci. 158 (1985) 103–125.
[76] W.R. Holland, D.G. Hall, Waveguide mode enhancement of molecular fluorescence, Optics Lett. 10 (1985) 414–416.
[77] J. Zhang, Y. Fu, J.R. Lakowicz, Emission behavior of fluorescently labeled silver nanoshell: enhanced self-quenching by metal nanostructure, J. Phys. Chem. C 111 (2007) 1955–1961.
[78] J.R. Lakowicz, J. Malicka, S.D. Auria, I. Gryczynski, Release of the self-quenching of fluorescence near silver metallic surfaces, Anal. Biochem. 320 (2003) 13–20.
[79] R.L. Stoermer, C.D. Keating, Distance-dependent emission from dye-labeled oligonucleotides on striped Au/Ag nanowires: effect of secondary structure and hybridization efficiency, J. Am. Chem. Soc. 128 (2006) 13243–13254.
[80] K. Ray, R. Badugu, J.R. Lakowicz, Distance-dependent metal-enhanced fluorescence from Langmuir–Blodgett monolayers of alkyl-NBD derivatives on silver island films, Langmuir 22 (2006) 8374–8378.

[81] G.V. Heijne, A day in the life of Dr. K or how I learned to stop worrying and love lysozyme, a tragedy in six acts, J. Mol. Biol. 293 (1999) 367–379.
[82] J. Zhang, Y. Fu, D. Liang, R.Y. Zhao, J.R. Lakowicz, Enhanced fluorescence images for labeled cells on silver island films, Langmuir 24 (2008) 12452–12457.
[83] X.F. Gu, T. Qiu, W.J. Zhang, P.K. Chu, Light emitting diodes Enhanced by localized surface plasmon resonance, Nanoscale Res. Lett. 6 (2011) 199.
[84] S. Kubo, Z.Z. Gu, D.A. Tryk, Y. Ohko, O. Sato, A. Fujishima, Metal-coated colloidal crystal film as surface-enhanced Raman scattering substrate, Langmuir 18 (2002) 5043–5046.
[85] D.M. Kuncicky, B.G. Prevo, O.D. Velev, Controlled assembly of SERS substrates templated by colloidal crystal films, J. Mater. Chem. 16 (2006) 1207–1211.
[86] F. Yu, S.J. Tian, D.F. Yao, W. Knoll, Surface Plasmon enhanced diffraction for label-free biosensing, Anal. Chem. 76 (2004) 3530–3535.
[87] T.W. Ebbesen, H.J. Lezec, H.F. Ghaemi, T. Thio, P.A. Wolf, Extraordinary optical transmission through sub-wavelength hole array, Nature 391 (1998) 667–669.
[88] C.P. Collier, T. Vossmeyer, J.R. Heath, Nanocrystal superlattices, Annu. Rev. Phys. Chem. 49 (1998) 371–404.
[89] S.I. Stoeva, B.L.V. Prasad, S. Uma, P.K. Stoimenov, V. Zaikovski, C.M. Sorensen, K.J. Klabunde, Face-centered cubic and hexagonal closed-packed nanocrystal superlattices of gold nanoparticles prepared by different methods, J. Phys. Chem. B 107 (2003) 7441–7448.
[90] Y. Yin, A.P. Alivisatos, Colloidal nanocrystal synthesis and the organic–inorganic interface, Nature 437 (2005) 664–670.
[91] C. Burda, X. Chen, R. Narayanan, M.A. El-Sayed, Chemistry and properties of nanocrystals of different shapes, Chem. Rev. 105 (2005) 1025–1102.
[92] R.J. Macfarlane, B. Lee, M.R. Jones, N. Harris, G.C. Schatz, C.A. Mirkin, Nanoparticle superlattice engineering with DNA, Science 334 (2011) 204–208.
[93] T. Qiu, X.L. Wu, Y.C. Cheng, G.G. Siu, P.K. Chu, Silver nanocrystal superlattices: self-assembly and optical emission, Appl. Phys. Lett. 88 (2006) 143111.
[94] T. Qiu, X.L. Wu, J.C. Shen, P.K. Chu, Silver nanocrystal superlattice coating for molecular sensing by surface-enhanced Raman spectroscopy, Appl. Phys. Lett. 89 (2006) 131914.
[95] T. Ito, S. Okazaki, Pushing the limits of lithography, Nature 406 (2000) 1027–1031.
[96] Q.M. Yu, P. Guan, D. Qin, G. Golden, P.M. Wallace, Inverted size-dependence of surface-enhanced Raman scattering on gold nanohole and nanodisk arrays, Nano Lett. 8 (2008) 1923–1928.
[97] J.C. Hulteen, R.P. Van Duyne, Nanosphere lithography – a materials general fabrication process for periodic particle array surfaces, J. Vac. Sci. Technol. A 13 (1995) 1553–1558.
[98] T.R. Jensen, G.C. Schatz, R.P. Van Duyne, Nanosphere lithography: surface plasmon resonance spectrum of a periodic array of silver nanoparticles by ultraviolet–visible extinction spectroscopy and electrodynamic modeling, J. Phys. Chem. B 103 (1999) 2394–2401.
[99] J.C. Hulteen, D.A. Treichel, M.T. Smith, M.L. Duval, T.R. Jensen, R.P. Van Duyne, Nanosphere lithography: size-tunable silver nanoparticle and surface cluster arrays, J. Phys. Chem. B 103 (1999) 3854–3863.
[100] T.R. Jensen, M.D. Malinsky, C.L. Haynes, R.P. Van Duyne, Nanosphere lithography: tunable localized surface plasmon resonance spectra of silver nanoparticles, J. Phys. Chem. B 104 (2000) 10549–10556.
[101] C.L. Haynes, R.P. Van Duyne, Nanosphere lithography: a versatile nanofabrication tool for studies of size-dependent nanoparticle optics, J. Phys. Chem. B 105 (2001) 5599–5611.
[102] F. Keller, M.S. Hunter, D.L. Robinson, Structural features of oxide coatings on aluminum, J. Electrochem. Soc. 100 (1953) 411–419.
[103] J.P. O'Sullivan, G.C. Wood, The morphology and mechanism of formation of porous anodic films on aluminium, Proc. Roy. Soc. Lond. A 317 (1970) 511–543.
[104] Y. Xu, G.E. Thompson, G.C. Wood, Mechanism of anodic film growth on aluminium, Trans. Inst. Met. Finish. 63 (1985) 98–103.
[105] O. Jessensky, F. Müller, U. Gösele, Self-organized formation of hexagonal pore arrays in anodic alumina, Appl. Phys. Lett. 72 (1998) 1173–1175.
[106] H. Masuda, H. Yamada, M. Satoh, H. Asoh, M. Nakao, T. Tamamura, Highly ordered nanochannel-array architecture in anodic alumina, Appl. Phys. Lett. 71 (1997) 2770–2772.
[107] H. Masuda, M. Satoh, Fabrication of gold nanodot Aarray using anodic porous alumina as an evaporation mask, Jpn. J. Appl. Phys. 35 (1996) L126–L129 (Part 2).
[108] H. Asoh, K. Nishio, M. Nakao, T. Tamamura, H. Masuda, Conditions for fabrication of ideally ordered anodic porous alumina using pretextured Al, J. Electrochem. Soc. 148 (2001) B152–B156.
[109] H. Masuda, K. Fukuda, Ordered Metal Nanohole Arrays made by a two-step replication of honeycomb structures of anodic alumina, Science 268 (1995) 1466–1468.
[110] C.H. Liu, J.A. Zapien, Y. Yao, X.M. Meng, C.S. Lee, S.S. Fan, Y. Lifshitz, S.T. Lee, High-density, ordered ultraviolet light-emitting ZnO nanowire arrays, Adv. Mater. 15 (2003) 838–841.
[111] K.K. Kim, J.I. Jin, Preparation of PPV nanotubes and nanorods and carbonized products derived Therefrom, Nano Lett. 1 (2001) 631–636.
[112] X.W. Wang, G.T. Fei, X.J. Xu, Z. Jin, L.D. Zhang, Size-dependent orientation growth of large-area ordered Ni nanowire arrays, J. Phys. Chem. B 109 (2005) 24326–24330.
[113] W.G. Jung, S.H. Jung, P. Kung, M. Razeghi, Fabrication of GaN nanotubular material using MOCVD with an aluminium oxide membrane, Nanotechnology 17 (2006) 54–59.
[114] T. Qiu, W.J. Zhang, X.Z. Lang, Y.J. Zhou, T.J. Cui, P.K. Chu, Controlled assembly of highly Raman-enhancing silver nanocap arrays templated by porous anodic alumina membranes, Small 5 (2009) 2333–2337.
[115] T. Qiu, F. Kong, X.Q. Yu, W.J. Zhang, X.Z. Lang, P.K. Chu, Tailoring light emission properties of organic emitter by coupling to resonance-tuned silver nanoantenna arrays, Appl. Phys. Lett. 95 (2009) 213104.

[116] K. Aslan, C.D. Geddes, Microwave-accelerated metal-enhanced fluorescence.platform technology for ultrafast and ultrabright assays, Anal. Chem. 77 (2005) 8057–8067.
[117] K.S. Phillips, Q. Cheng, Recent advances in surface plasmon resonance based techniques for bioanalysis, Anal. Bioanal. Chem. 387 (2007) 1831–1840.
[118] Y. Fu, J. Zhang, J.R. Lakowicz, Highly efficient detection of single fluorophores in blood serum samples with high autofluorescence, Photochem. Photobiol. 85 (2009) 646–651.
[119] T. Basche, W.E. Moerner, Optical modification of a single impurity molecule in a solid, Nature 355 (1992) 335–337.
[120] Y. Fu, J.R. Lakowicz, Enhanced single-molecule detection using porous silver membrane, J. Phys. Chem. C 114 (2010) 7492–7495.
[121] S. Henikoff, Unidirectional digestion with exonuclease III creates targeted breakpoints for DNA sequencing, Gene 28 (1984) 351–359.
[122] J. Zhang, Y. Fu, D. Liang, K. Nowaczyk, R.Y. Zhao, J.R. Lakowicz, Single-cell fluorescence imaging using metal plasmon-coupled probe 2: single-molecule counting on lifetime image, Nano Lett. 8 (2008) 1179.
[123] J. Zhang, Y. Fu, D. Liang, R.Y. Zhao, J.R. Lakowicz, Fluorescent avidin-bound silver particle: a strategy for single target molecule detection on a cell membrane, Anal. Chem. 81 (2009) 883–889.
[124] D. Osella, P. Pollone, M. Ravera, M. Salmain, G. Jaouen, Use of heavy-metal clusters in the design of *n*-succinimidyl ester acylation reagents for side-chain-specific labeling of proteins, Bioconjug. Chem. 10 (1999) 607–612.
[125] R.D. Smiley, G.G. Hammes, Single molecule studies of enzyme mechanisms, Chem. Rev. 106 (2006) 3080–3094.
[126] C. Xie, F. Xu, X. Huang, Single gold nanoparticles counter: an ultrasensitive detection platform for one-step homogeneous immunoassays and DNA hybridization assays, J. Am. Chem. Soc. 131 (2009) 12763–12770.
[127] J.R. Wayment, J.M. Harris, Biotin-Avidin binding kinetics measured by single-molecule imaging, Anal. Chem. 81 (2009) 336–342.
[128] J. Zhang, Y. Fu, Y. Mei, F. Jiang, J.R. Lakowicz, Fluorescent metal nanoshell probe to detect single miRNA in lung cancer cell, Anal. Chem. 82 (2010) 4464–4471.
[129] Y. Fu, J. Zhang, J.R. Lakowicz, Metal-enhanced fluorescence of single green fluorescent protein (GFP), Biochem. Bioph. Res. Co. 376 (2008) 712–717.
[130] K. Ray, M.H. Chowdhury, J.R. Lakowicz, Single-molecule spectroscopic study of enhanced intrinsic phycoerythrin fluorescence on silver nanostructured surfaces, Anal. Chem. 80 (2008) 6942–6948.
[131] X. Cui, K. Tawa, H. Hori, J. Nishii, Tailored plasmonic gratings for enhanced fluorescence detection and microscopic imaging, Adv. Funct. Mater. 20 (2010) 546–553.
[132] A. Giannattasio, I.R. Hooper, W.L. Barnes, Dependence on surface profile in grating-assisted coupling of light to surface plasmon-polaritons, Opt. Commun. 261 (2006) 291–295.
[133] M. Bruchez, M. Moronne, P. Gin, S. Weiss, A.P. Alivisatos, Semiconductor nanocrystals as fluorescent biological labels, Science 281 (1998) 2013–2016.
[134] K.T. Shimizu, W.K. Woo, B.R. Fisher, H.J. Eisler, M.G. Bawendi, Surface-enhanced emission from single semiconductor nanocrystals, Phys. Rev. Lett. 89 (2002) 117401–117405.
[135] O. Kulakovich, N. Strekal, A. Yaroshevich, S. Maskevich, S. Gaponenko, I. Nabiev, U. Woggon, M. Artemyev, Enhanced luminescence of CdSe quantum dots on gold colloids, Nano Lett. 2 (2002) 1449–1452.
[136] E. Katz, I. Willner, Integrated nanoparticle–biomolecule hybrid systems: synthesis, properties, and applications, Angew. Chem. Int. Ed. 43 (2004) 6042–6108.
[137] N.R. Jana, Gram-scale synthesis of soluble, near-monodisperse gold nanorods and other anisotropic nanoparticles, Small 1 (2005) 875–882.
[138] S.I. Stoeva, J.S. Lee, J.E. Smith, S.T. Rosen, C.A. Mirkin, Multiplexed detection of protein cancer markers with biobarcoded nanoparticle probes, J. Am. Chem. Soc. 128 (2006) 8378–8379.
[139] P.K. Jain, X. Huang, I.H. El-Sayed, M.A. El-Sayed, Noble metals on the nanoscale: optical and photothermal properties and some applications in imaging, sensing, biology, and medicine, Acc. Chem. Res. 41 (2008) 1578–1586.
[140] J. Kim, H.S. Kim, N. Lee, T. Kim, H. Kim, T. Yu, I.C. Song, W.K. Moon, T. Hyeon, Multifunctional uniform nanoparticles composed of a magnetite nanocrystal core and a mesoporous silica shell for magnetic resonance and fluorescence imaging and for drug delivery, Angew. Chem. Int. Edit. 120 (2008) 8566–8569.
[141] J. Enderlein, Spectral properties of a fluorescing moleculewithin a spherical metallic cavity, Phys. Chem. Chem. Phys. 4 (2002) 2780–2786.
[142] J. Enderlien, Theoretical study of single molecule fluorescence in a metallic nanocavity, Appl. Phys. Lett. 80 (2002) 315–317.
[143] N. Liu, B.S. Prall, V.I. Klimov, Hybrid gold/silica/nanocrystal-quantum-dot superstructures: synthesis and analysis of semiconductor-metal interactions, J. Am. Chem. Soc. 128 (2006) 15362–15363.
[144] K. Ray, R. Badugu, J.R. Lakowicz, Metal-enhanced fluorescence from CdTe nanocrystals: a single-molecule fluorescence study, J. Am. Chem. Soc. 128 (2006) 8998–8999.
[145] T. Pons, I.L. Medintz, K.E. Sapsford, S. Higashiya, A.F. Grimes, D.S. English, H. Mattoussi, On the quenching of semiconductor quantum dot photoluminescence by proximal gold nanoparticles, Nano Lett. 7 (2007) 3157–3164.
[146] A. Saha, S.K. Basiruddin, R. Sarkar, N. Pradhan, N.R. Jana, Functionalized plasmonic-fluorescent nanoparticles for imaging and detection, J. Phys. Chem. C 113 (2009) 18492–18498.
[147] J. Zenneck, Über die fortpflanzung ebener elektromagnetischer wellen langs einer ebenen leiterflache und ihre beziehung zur drahtlosen telegraphie, Ann. Phys-berlin Ann. Phys. 328 (1907) 846–866.
[148] R.H. Ritchie, Plasma losses by fast electrons in thin films, Phys. Rev. 106 (1957) 874–881.
[149] M. Fleischmann, P.J. Hendra, A.J. McQuillan, Raman spectra of pyridine adsorbed at a silver electrode, Chem. Phys. Lett. 26 (1974) 163–166.
[150] J. Chan, S. Fore, S.W. Hogiu, T. Huser, Raman spectroscopy and microscopy of individual cells and cellular components, Laser Photonics Rev. 2 (2008) 325–349.
[151] M. Kazanci, H.D. Wagner, N.I. Manjubala, H.S. Gupta, E. Paschalis, P. Roschger, P. Fratzl, Raman imaging of two orthogonal planes within cortical bone, Bone 41 (2007) 456–461.

[152] G.J. Zhang, D.J. Moore, C.R. Flach, R. Mendelsohn, Vibrational microscopy and imaging of skin: from single cells to intact tissue: from single cells to intact tissue, Anal. Bioanal. Chem. 387 (2007) 1591–1599.
[153] G.J. Zhang, D.J. Moore, K.B. Sloan, C.R. Flach, R. Mendelsohn, Imaging the prodrug-to-drug transformation of a 5-fluorouracil derivative in skin by confocal Raman microscopy, J. Investig. Dermatol. 127 (2007) 1205–1209.
[154] O. Schiemann, T.F. Prisner, Long-range distance determinations in biomacromolecules by EPR spectroscopy, Q. Rev. Biophys. 40 (2007) 1–53.
[155] J.R. Lakowicz, Plasmonics in biology and plasmon-controlled fluorescence, Plasmonics 1 (2006) 5–33.
[156] J.B. Pawley, Handbook of Biological Confocal Microscopy, second ed., Plenum Press, New York, 1995.